Supplementary Information

Photoactive glycoconjugates with very large Stokes shift. Synthesis, photophysics, and copper (II) and BSA sensing

Cláudia Brito da Silva,[a] Luana Silva,[b] Natalí Pires Debia,[b] Otávio Augusto Chaves,[c,d] Diogo Seibert Lüdtke*[b] and Fabiano Severo Rodembusch*[a]

[a]Grupo de Pesquisa em Fotoquímica Orgânica Aplicada. Instituto de Química (UFRGS), Av. Bento Gonçalves, 9500, CEP 91501-970. Porto Alegre-RS, Brazil.
[b]Instituto de Química, Universidade Federal do Rio Grande do Sul, UFRGS, Av. Bento Gonçalves 9500, 91501-970 Porto Alegre, RS, Brazil.
[c]CQC-IMS, Departamento de Química, Universidade de Coimbra, Rua Larga, 3004-535 Coimbra, Portugal.
[d]Laboratório de Imunofarmacologia, Centro de Pesquisa, Inovação e Vigilância em COVID-19 e Emergências Sanitárias (CPIV), Instituto Oswaldo Cruz (IOC), Fundação Oswaldo Cruz (Fiocruz), Av. Brasil 4036 - Bloco 2, 21040-361 Rio de Janeiro – RJ, Brazil

Summary

Spectroscopic characterization

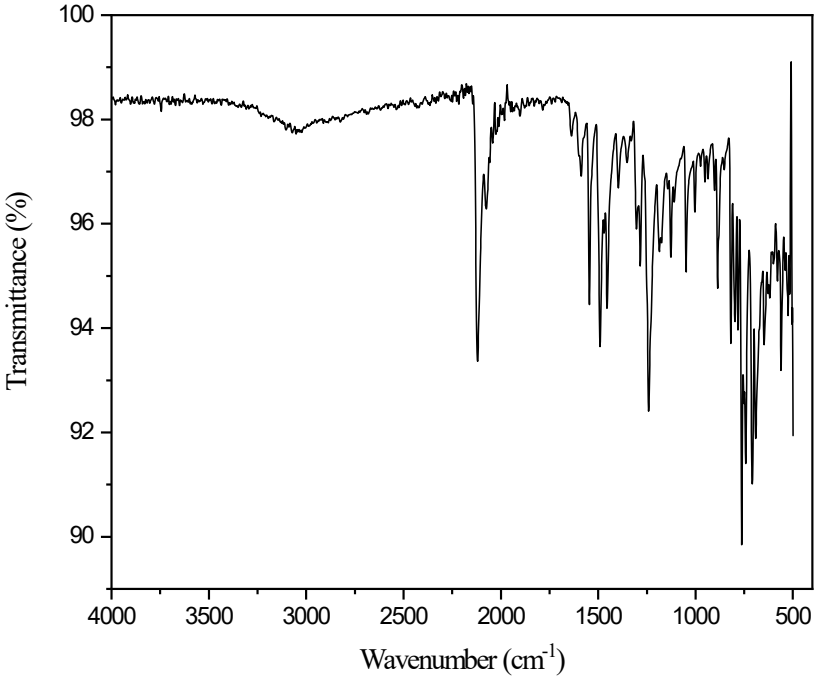

Fig. S1 FTIR spectrum (ATR mode) of compound **3**.

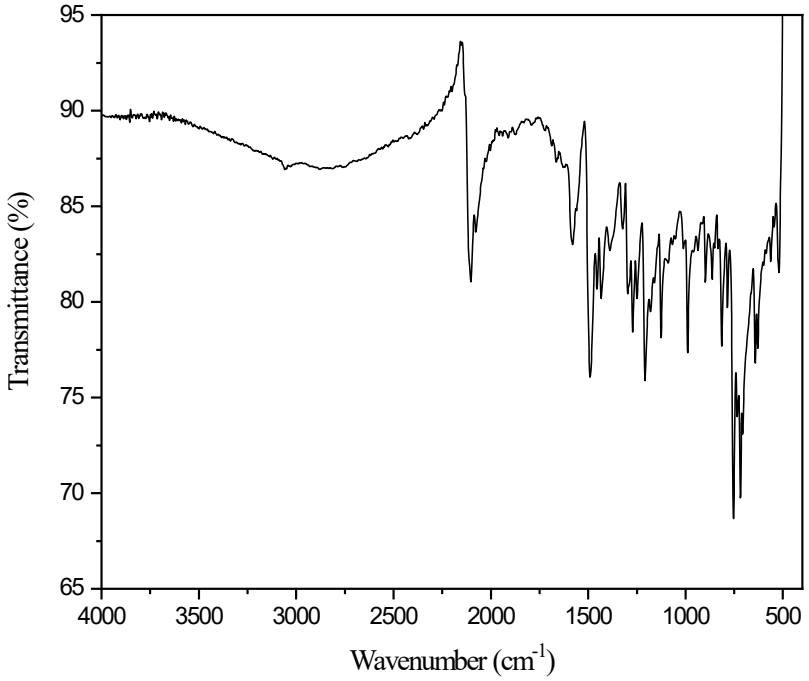

Fig. S2 FTIR spectrum (ATR mode) of compound **4**.

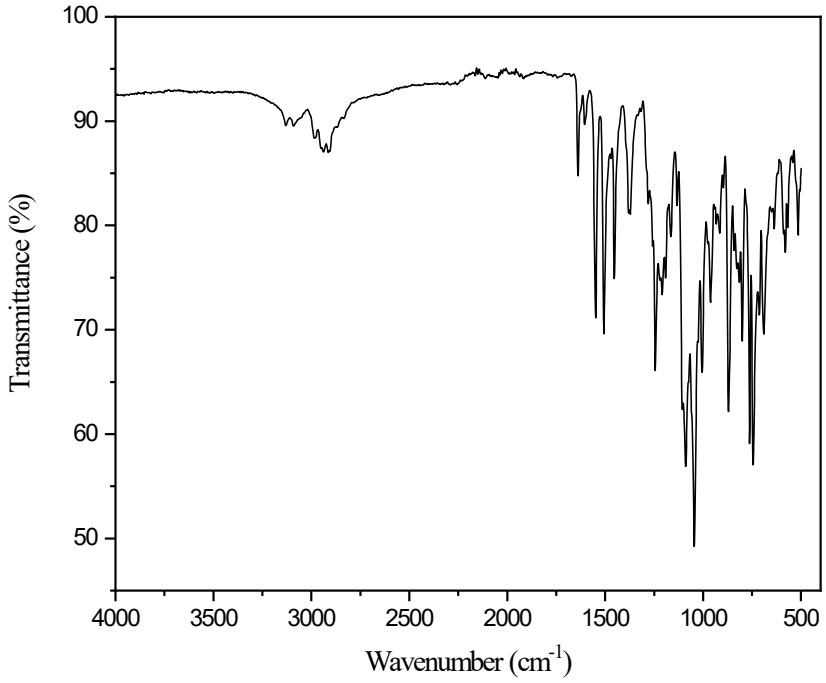

Fig. S3 FTIR spectrum (ATR mode) of compound **15**.

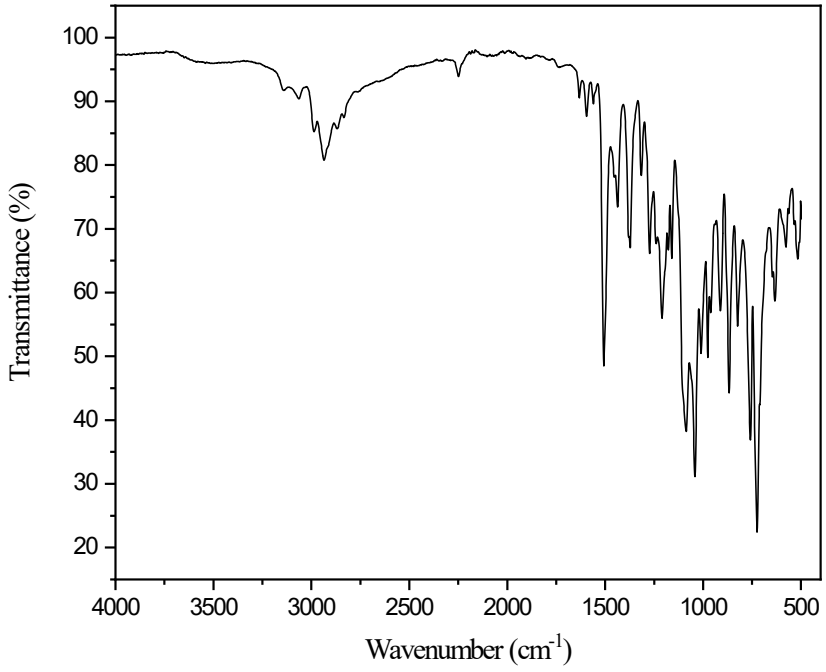

Fig. S4 FTIR spectrum (ATR mode) of compound **16**.

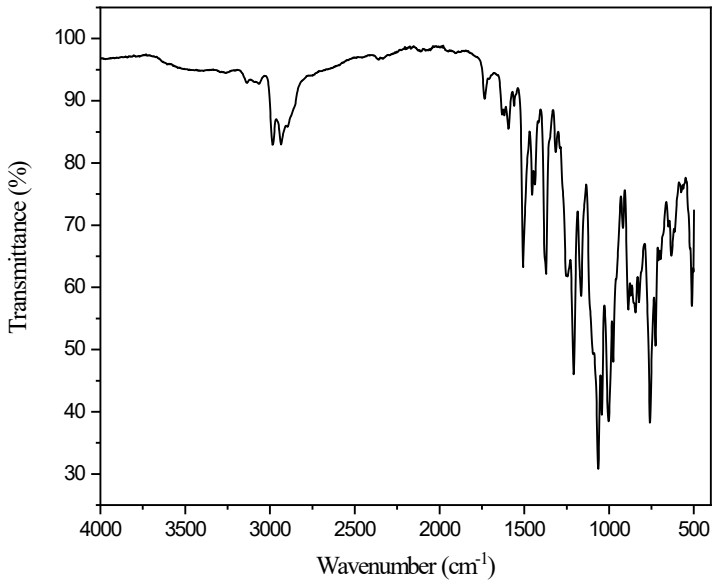

Fig. S5 FTIR spectrum (ATR mode) of compound **17**.

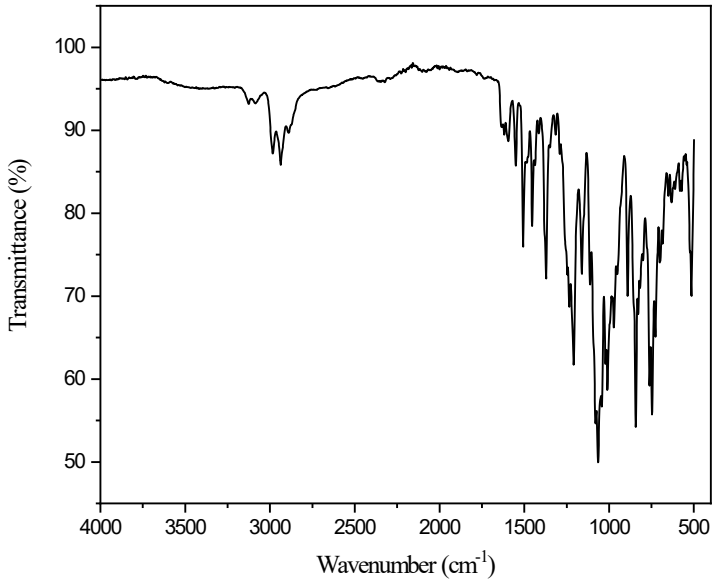

Fig. S6 FTIR spectrum (ATR mode) of compound **18**.

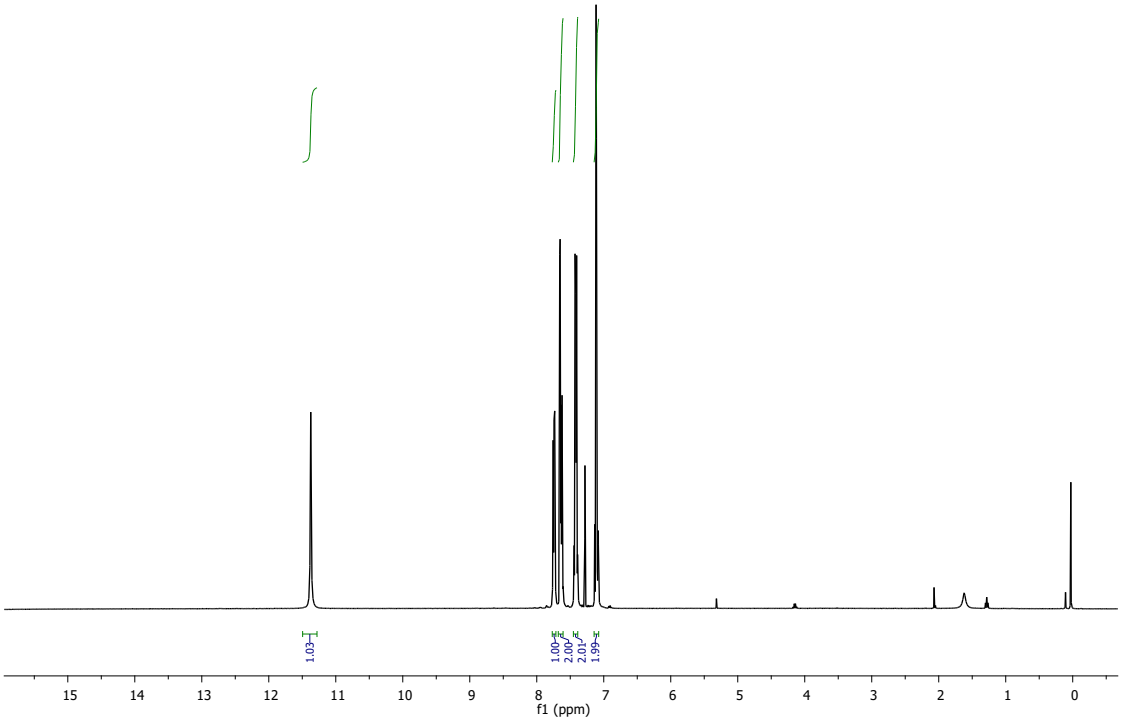

Fig. S7 ^{1}H NMR spectrum (400 MHz, $CDCl_3$) of compound **3**.

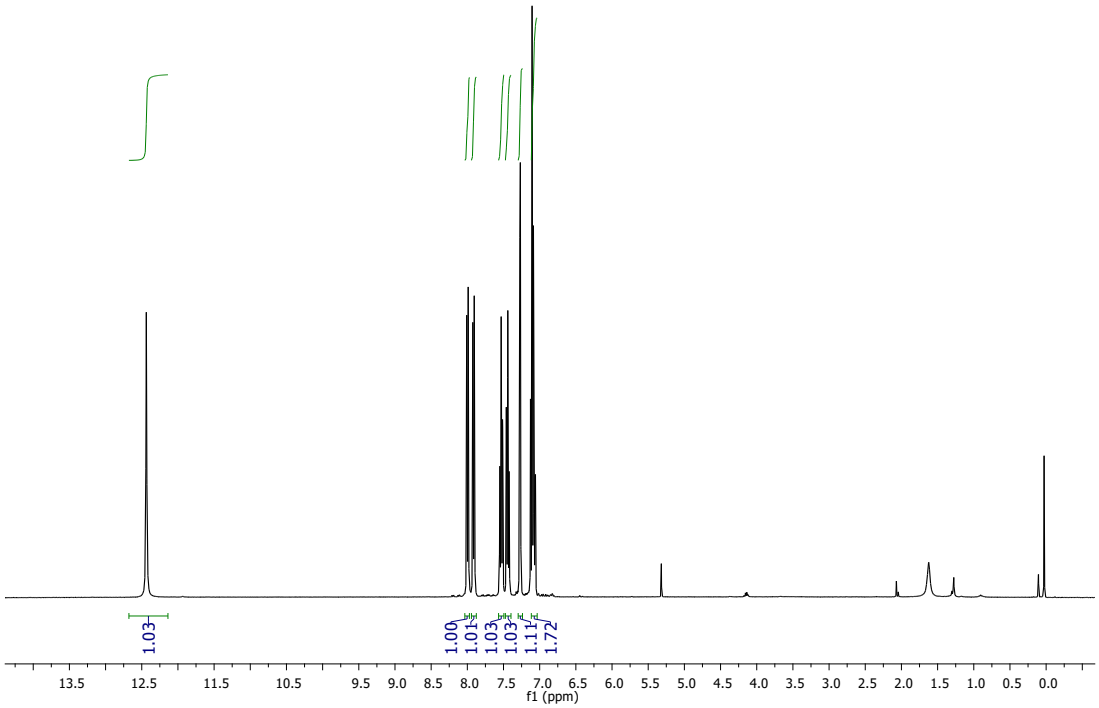

Fig. S8 ^{1}H NMR spectrum (400 MHz, $CDCl_3$) of compound **4**.

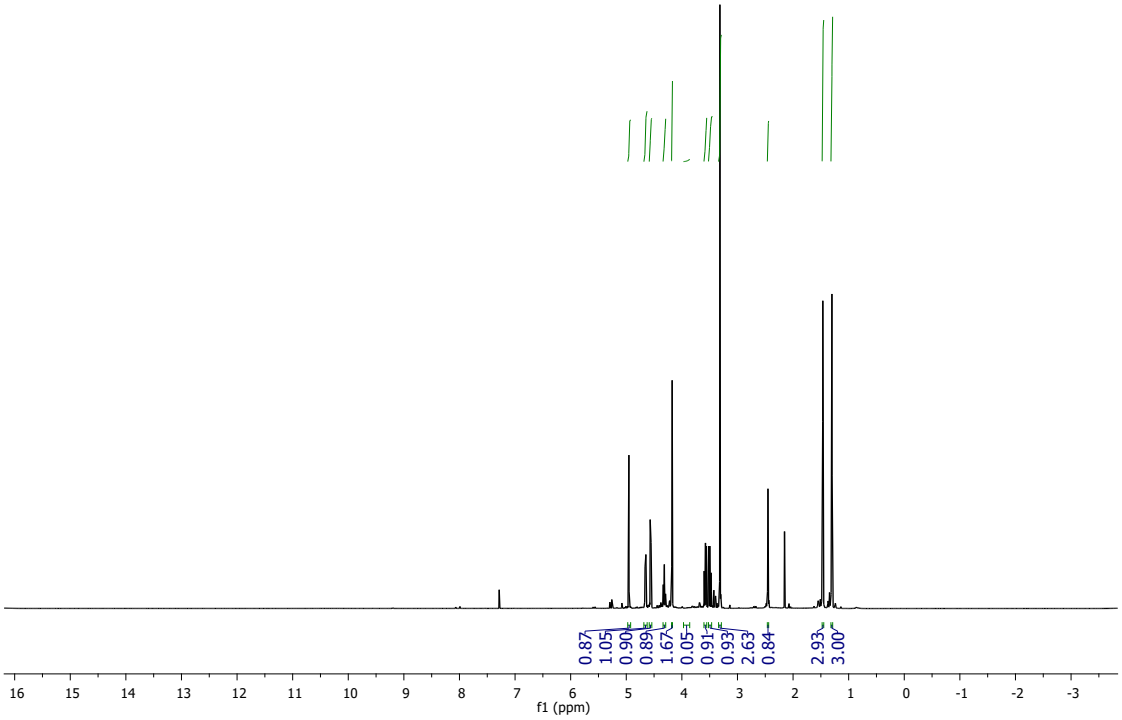

Fig. S9 ^{1}H NMR spectrum (400 MHz, $CDCl_3$) of compound **8**.

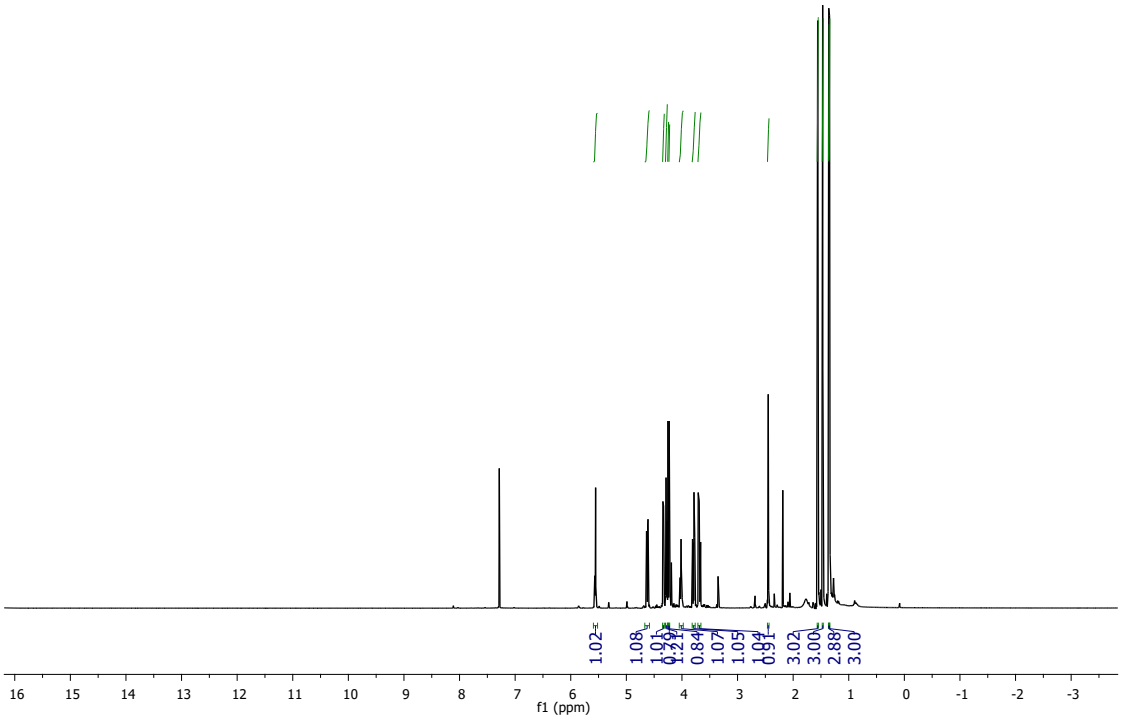

Fig. S10 ^{1}H NMR spectrum (400 MHz, $CDCl_3$) of compound **11**.

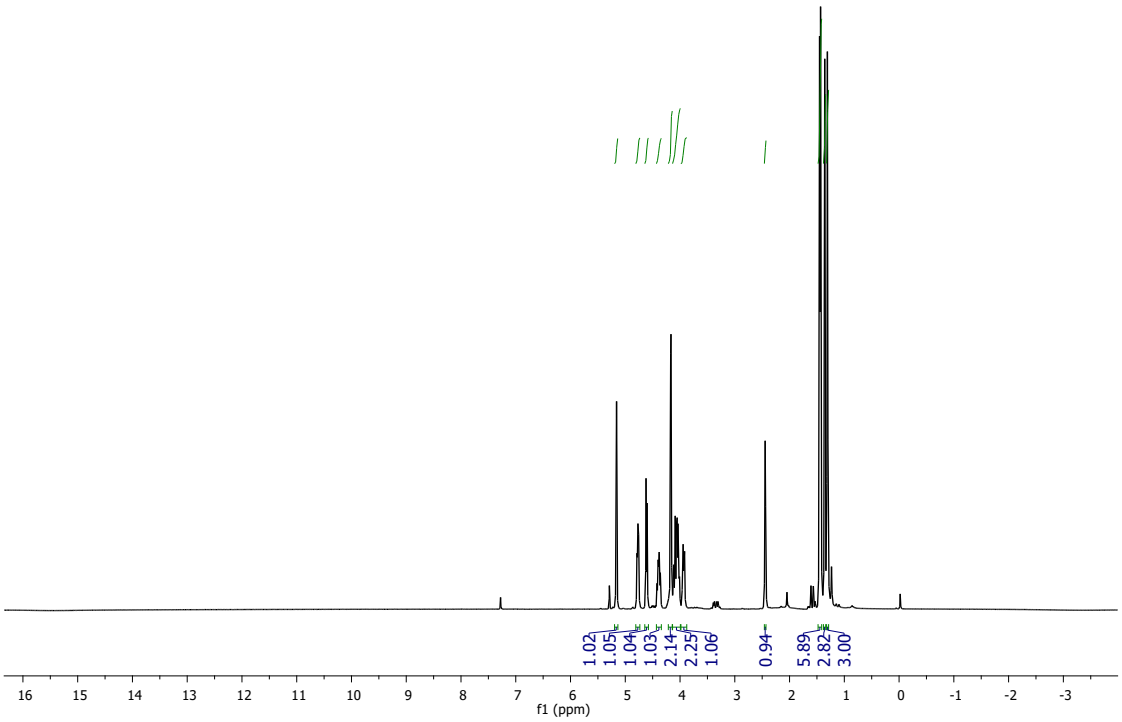

Fig. S11 ^{1}H NMR spectrum (400 MHz, $CDCl_3$) of compound **14**.

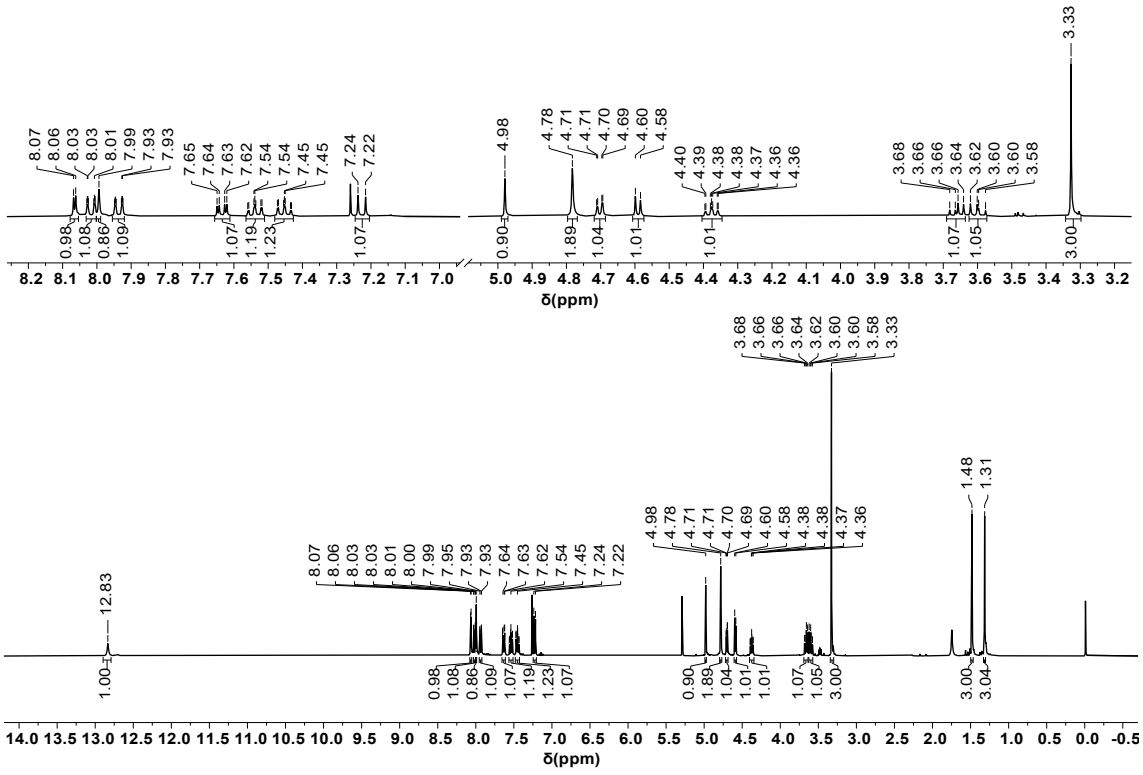

Fig. S12 ^{1}H NMR spectrum with amplification (400 MHz, $CDCl_3$) of compound **15**.

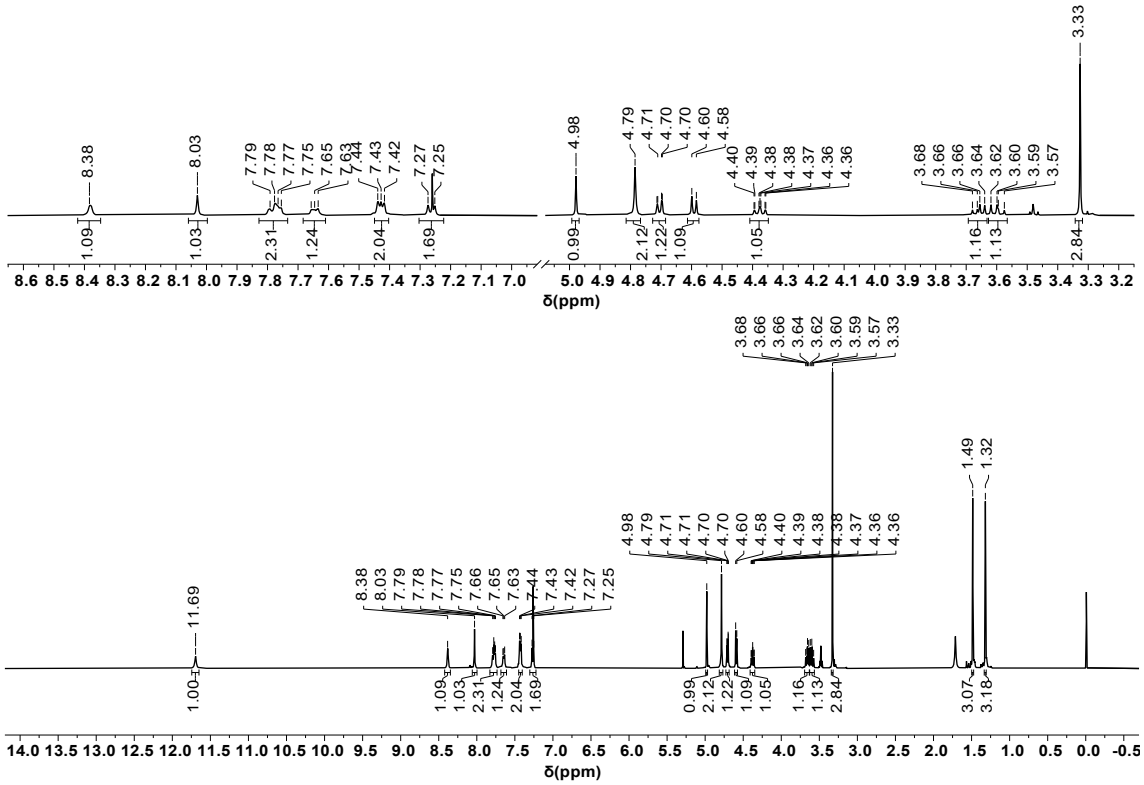

Fig. S13 ^{1}H NMR spectrum with amplification (400 MHz, $CDCl_3$) of compound **16**.

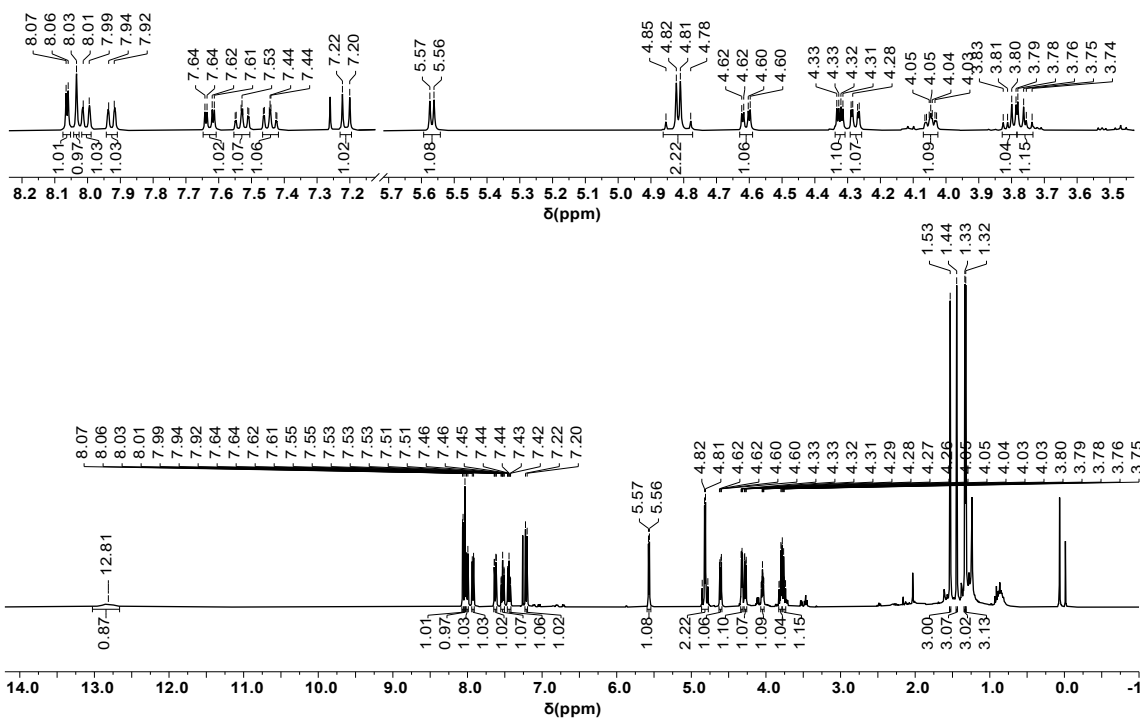

Fig. S14 ^{1}H NMR spectrum with amplification (400 MHz, $CDCl_3$) of compound **17**.

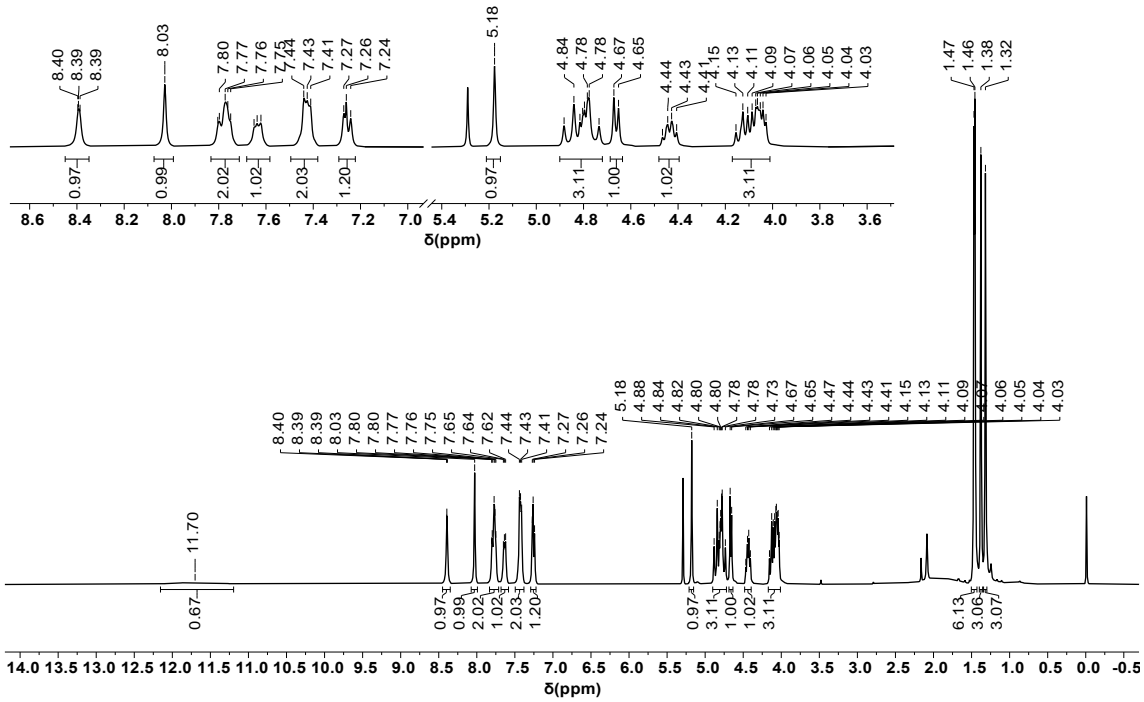

Fig. S15 ^{1}H NMR spectrum with amplification (400 MHz, $CDCl_3$) of compound **18**.

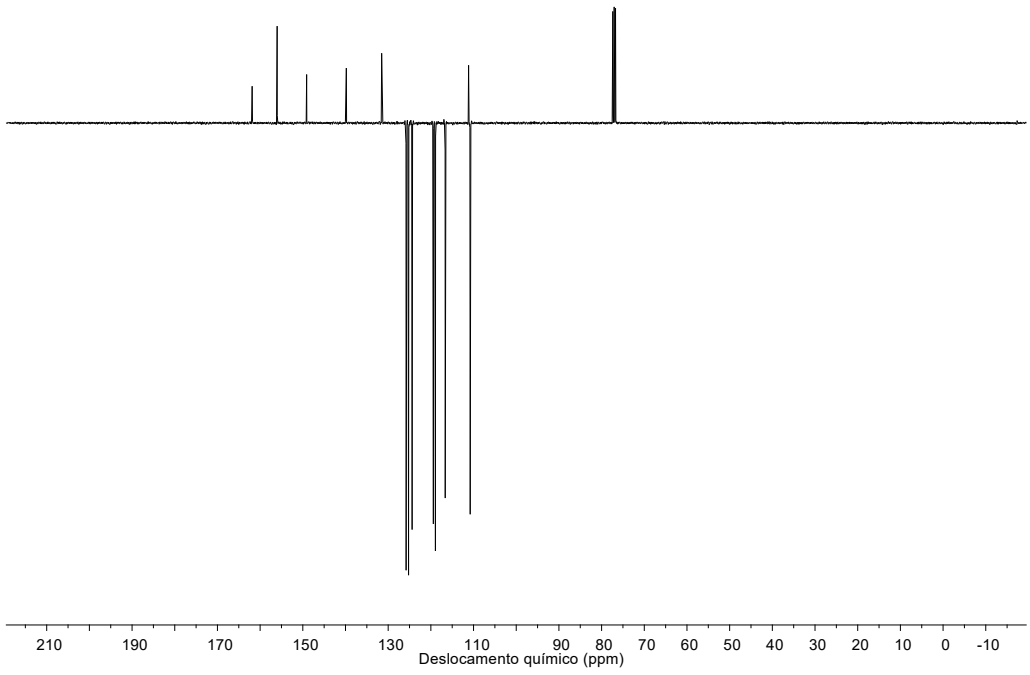

Fig. S16 ^{13}C-APT NMR spectrum (101 MHz, $CDCl_3$) of compound **3**.

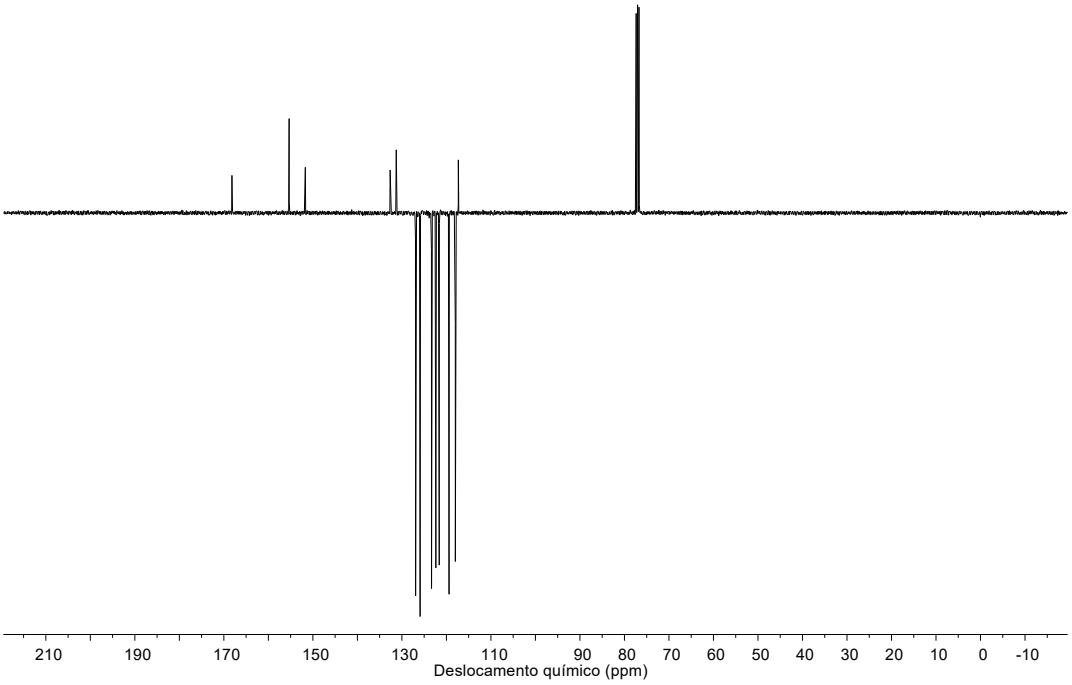

Fig. S17 ^{13}C-APT NMR spectrum (101 MHz, $CDCl_3$) of compound **4**.

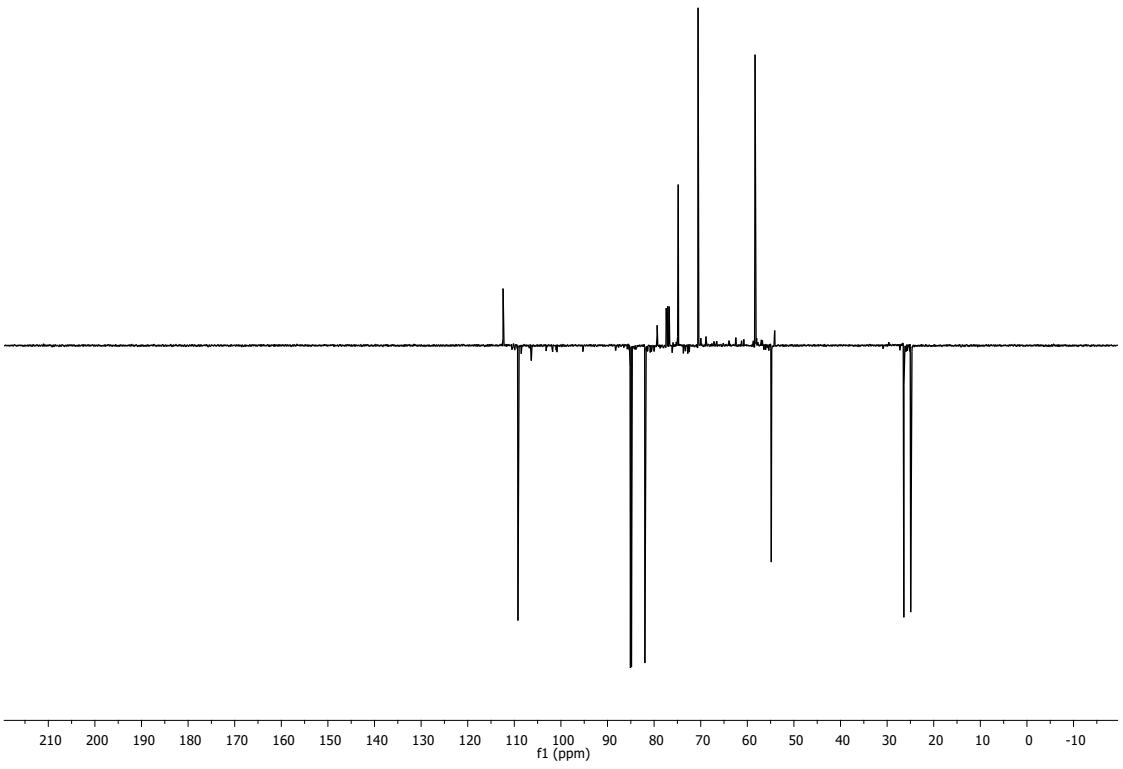

Fig. S18 ^{13}C-APT NMR spectrum (101 MHz, $CDCl_3$) of compound **8**.

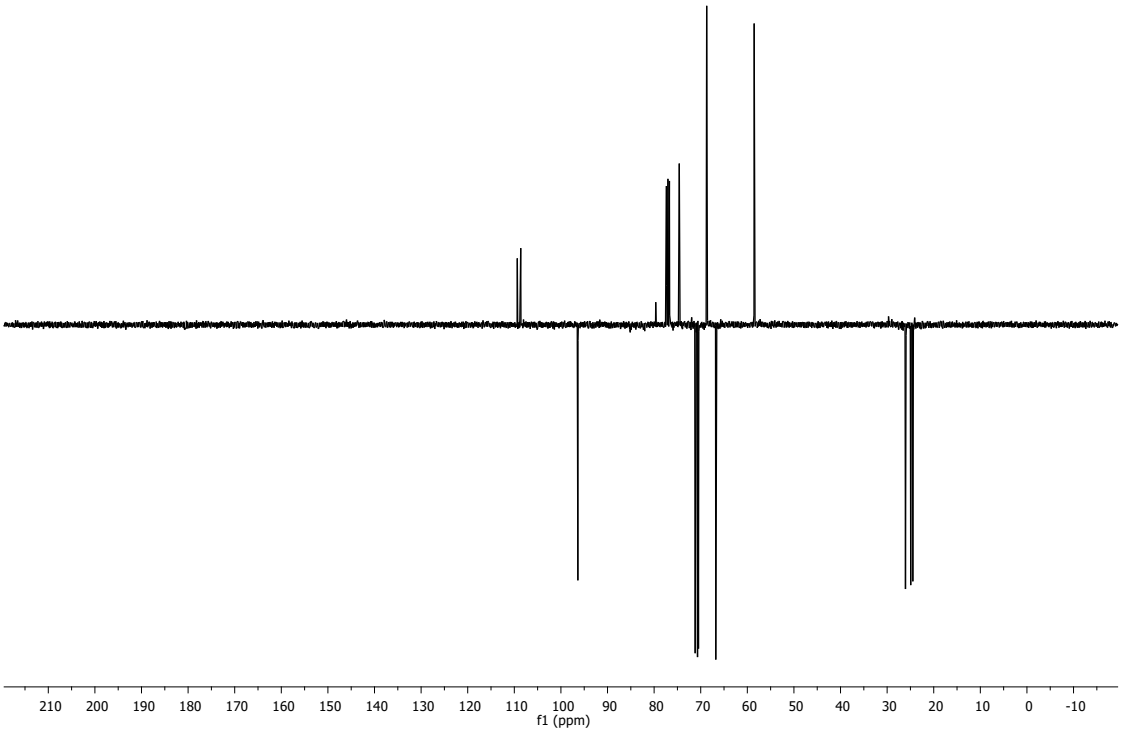

Fig. S19 ^{13}C-APT NMR spectrum (101 MHz, $CDCl_3$) of compound **11**.

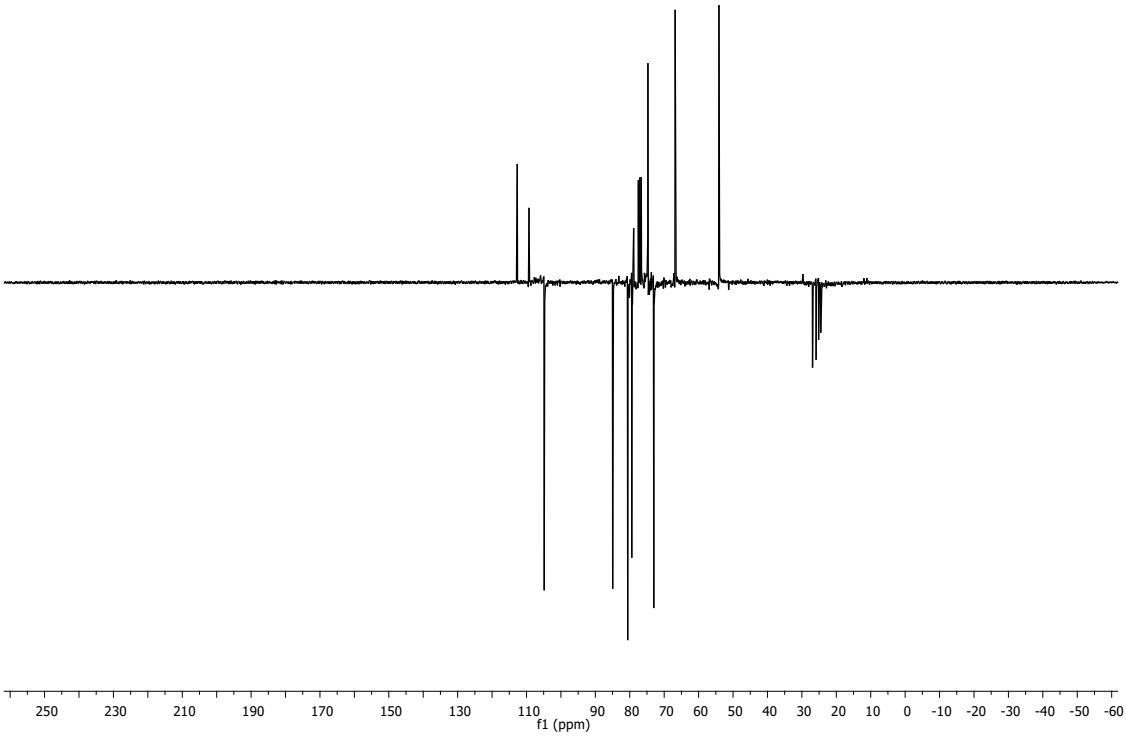

Fig. S20 ^{13}C-APT NMR spectrum (101 MHz, $CDCl_3$) of compound **14**.

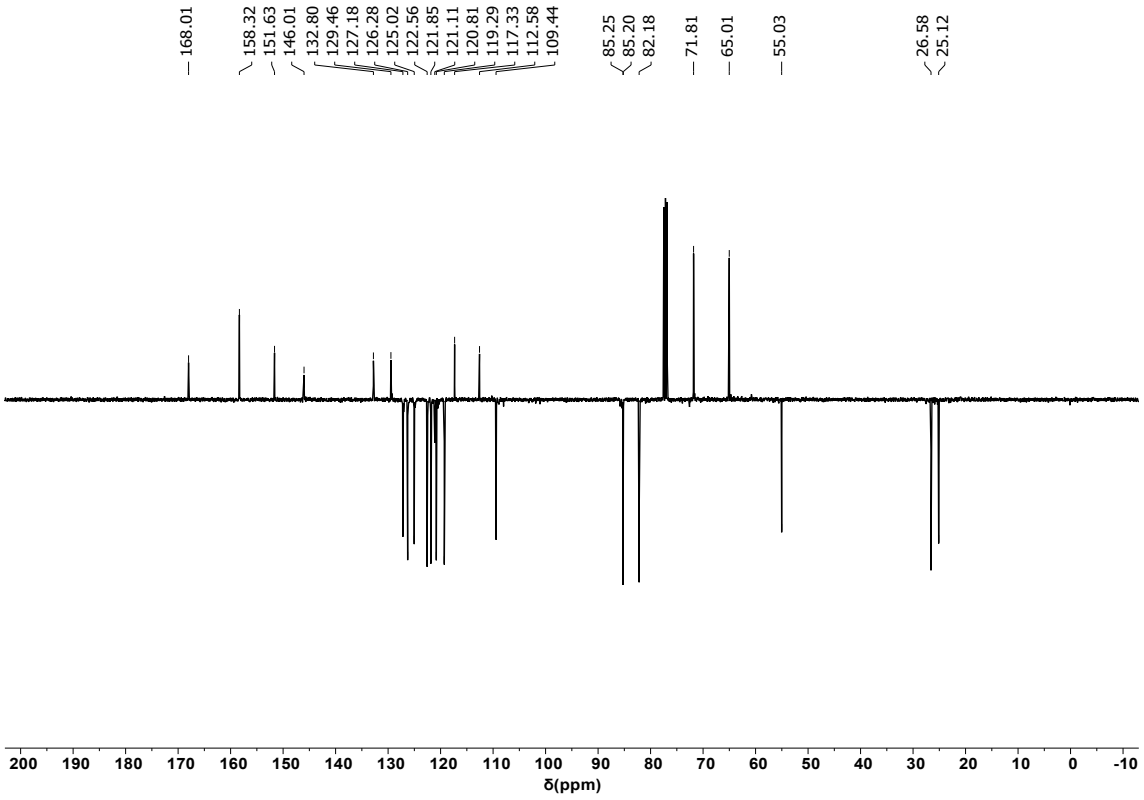

Fig. S21 ^{13}C-APT NMR spectrum (101 MHz, $CDCl_3$) of compound **15**.

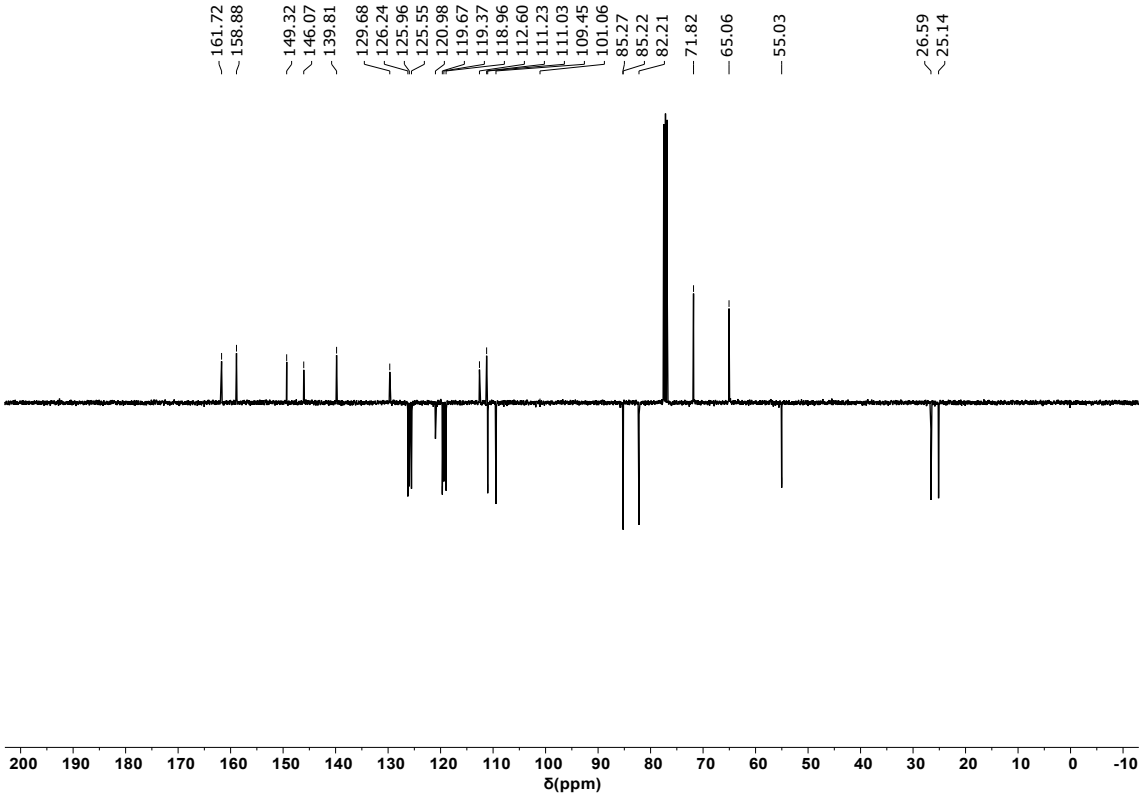

Fig. S22 ^{13}C-APT NMR spectrum (101 MHz, $CDCl_3$) of compound **16**.

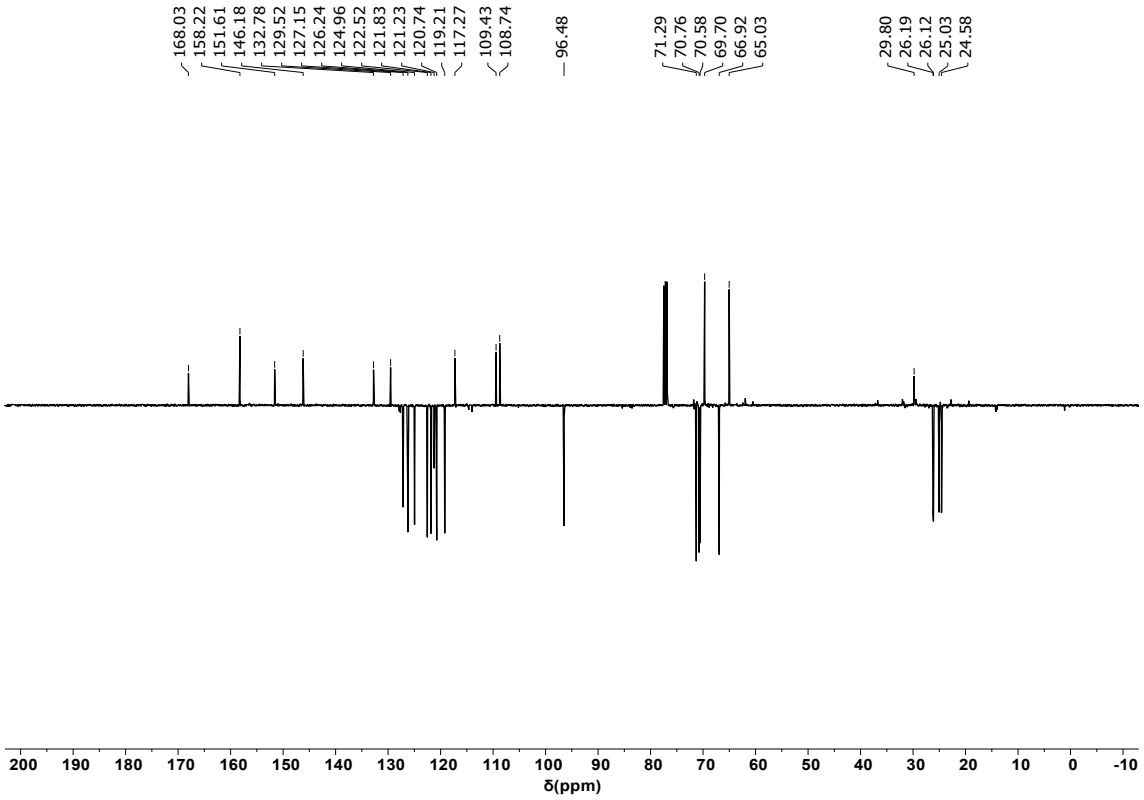

Fig. S23 ^{13}C-APT NMR spectrum (101 MHz, $CDCl_3$) of compound **17**.

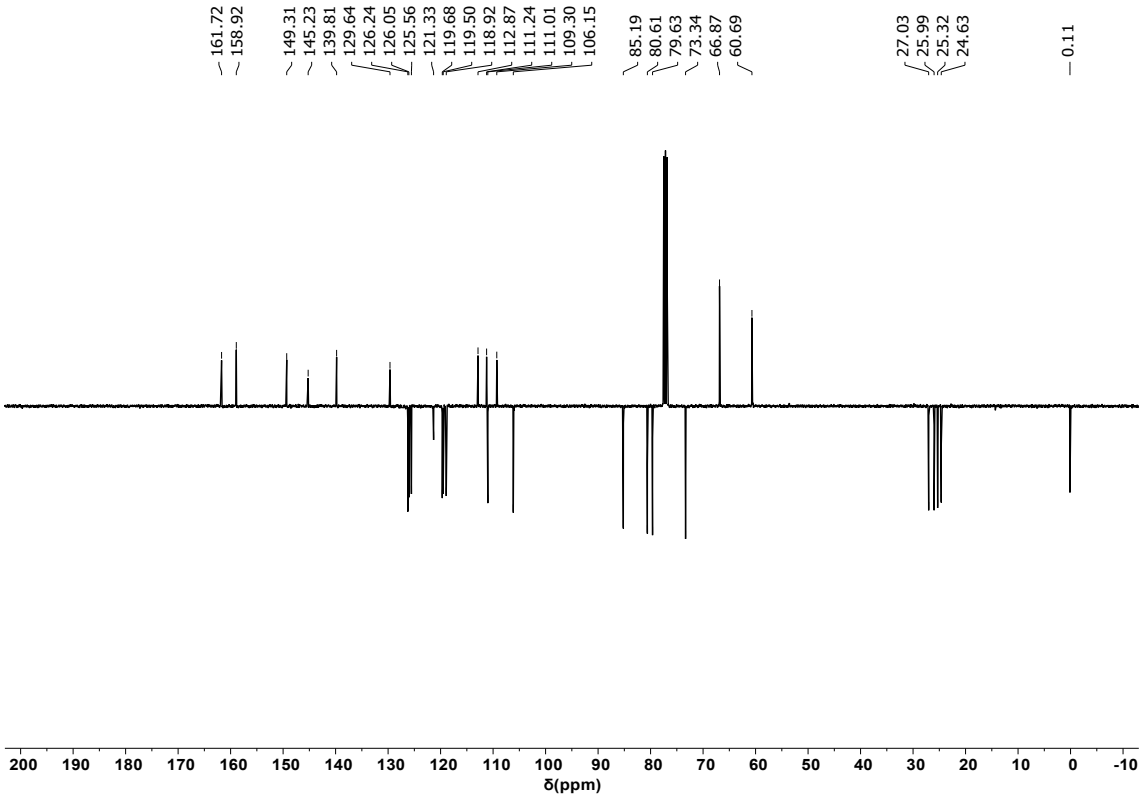

Fig. S24 ^{13}C-APT NMR spectrum (101 MHz, $CDCl_3$) of compound **18**.

Additional UV-Vis spectra

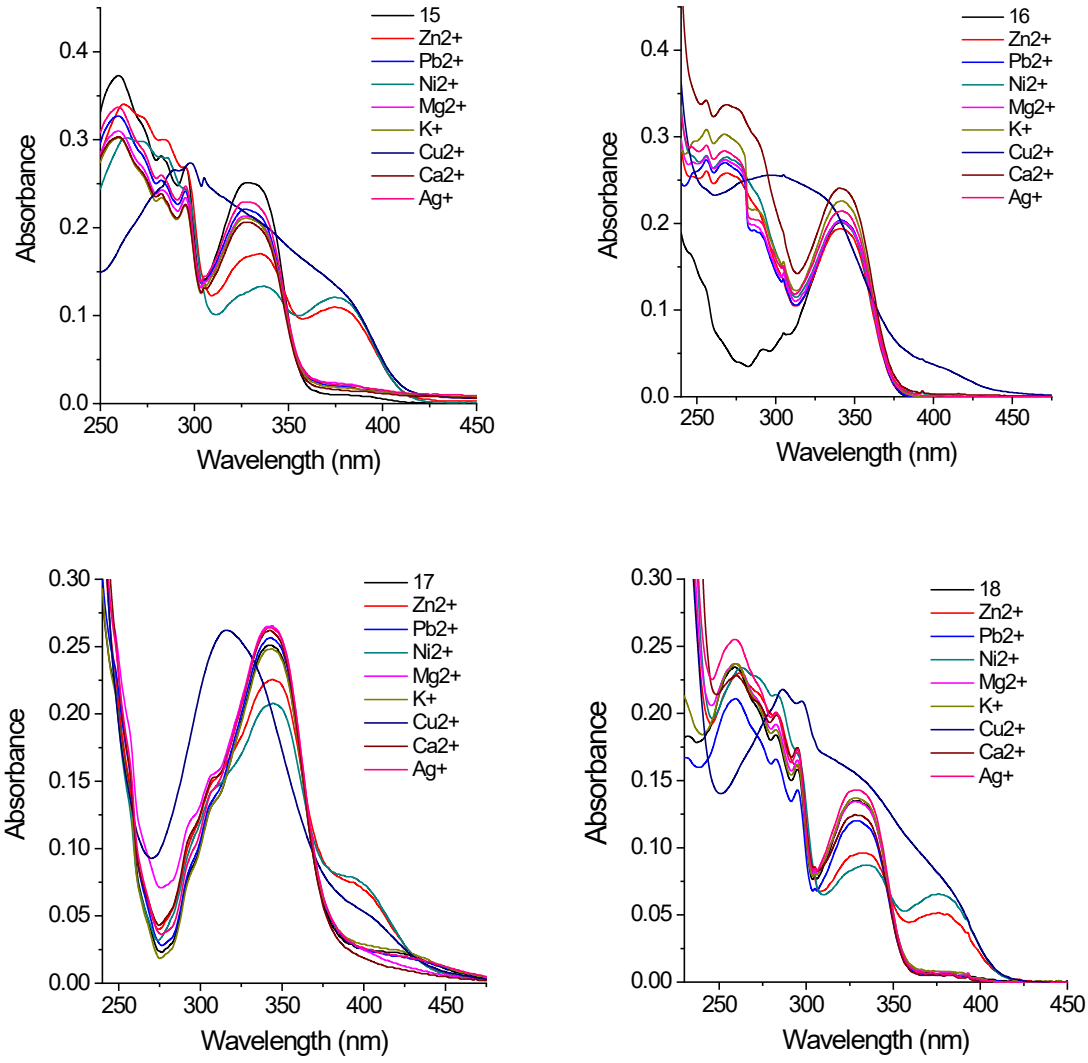

Fig. S25 UV-Vis absorption spectra of the glycoconjugates (a) **15**, (b) **16**, (c) **17**, and (d) **18** in the presence of different NO_3^- salts (20 equiv.).

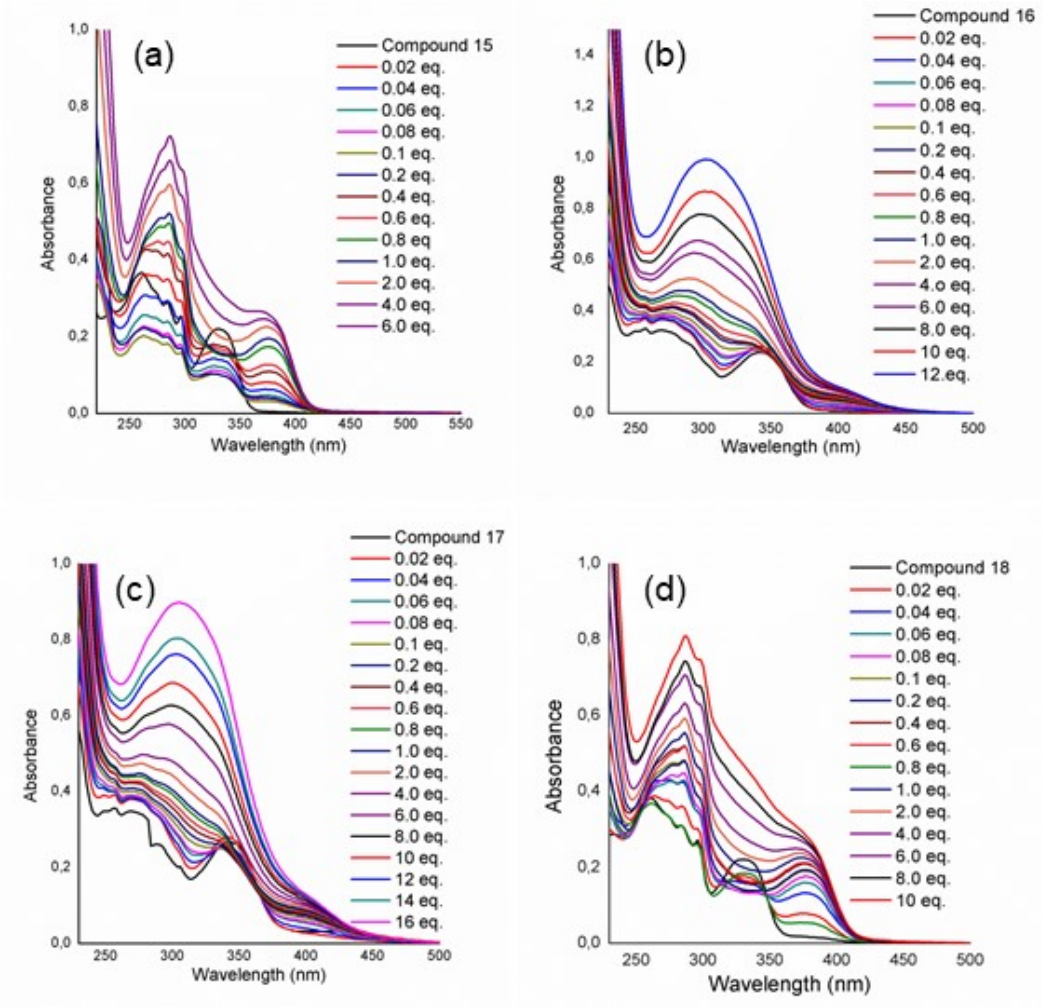

Fig. S26 UV-Vis absorption spectra of the glycoconjugates (a) **15**, (b) **16**, (c) **17**, and (d) **18** in the presence of different $Cu(NO_3)_2$ equivalents in acetonitrile solution,

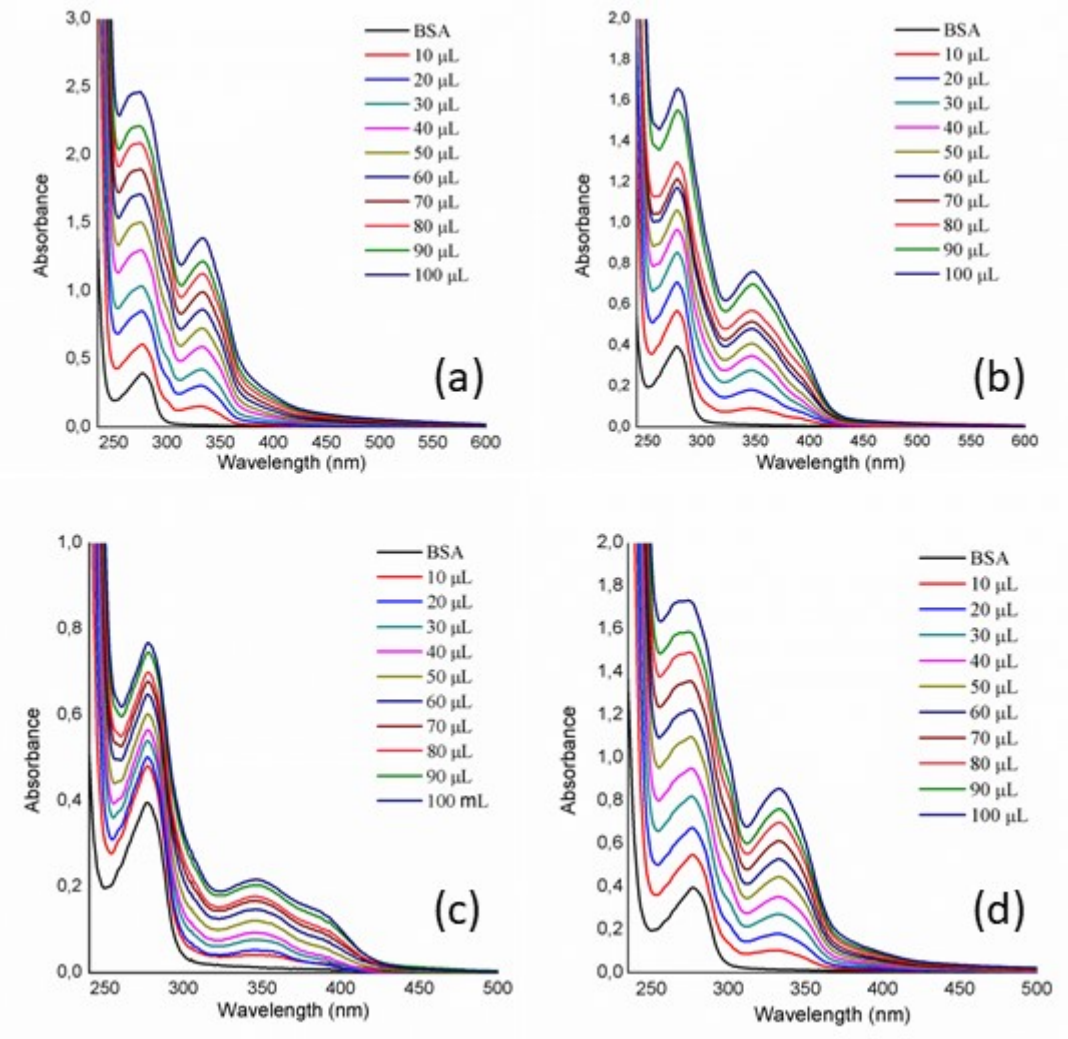

Fig. S27 UV-Vis absorption spectra of BSA in the presence of different concentrations of glycoconjugates (a) **15**, (b) **16**, (c) **17**, and (d) **18** (10-100 µM).

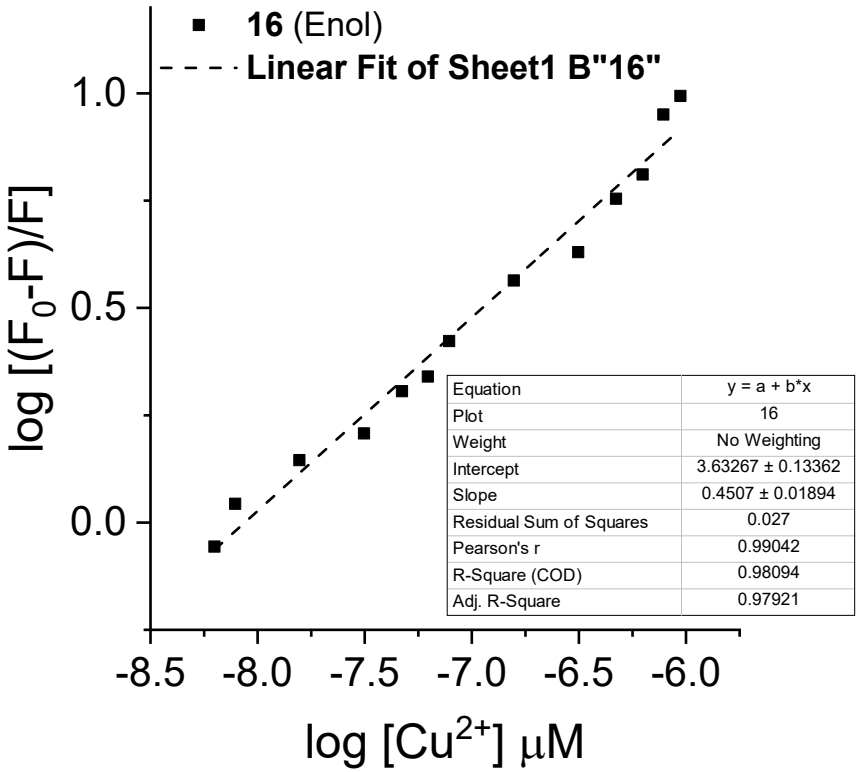

Fig. S28 Double logarithm plots for the K_a and *n* calculations of glycoconjugate **16** (enol).

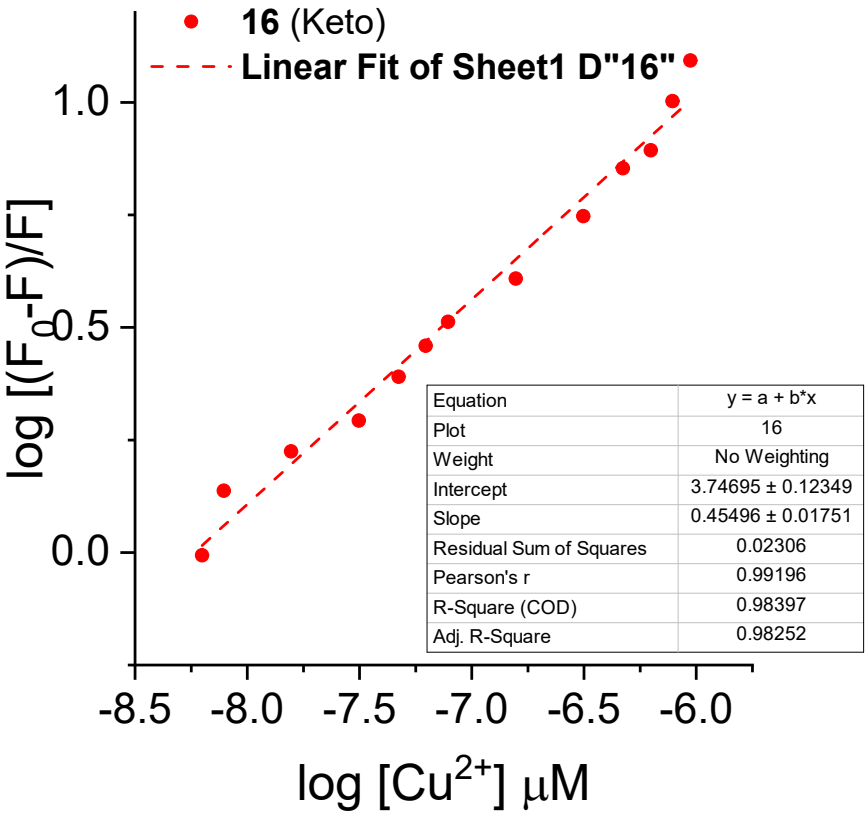

Fig. S29 Double logarithm plots for the K_a and *n* calculations of glycoconjugate **16** (keto).

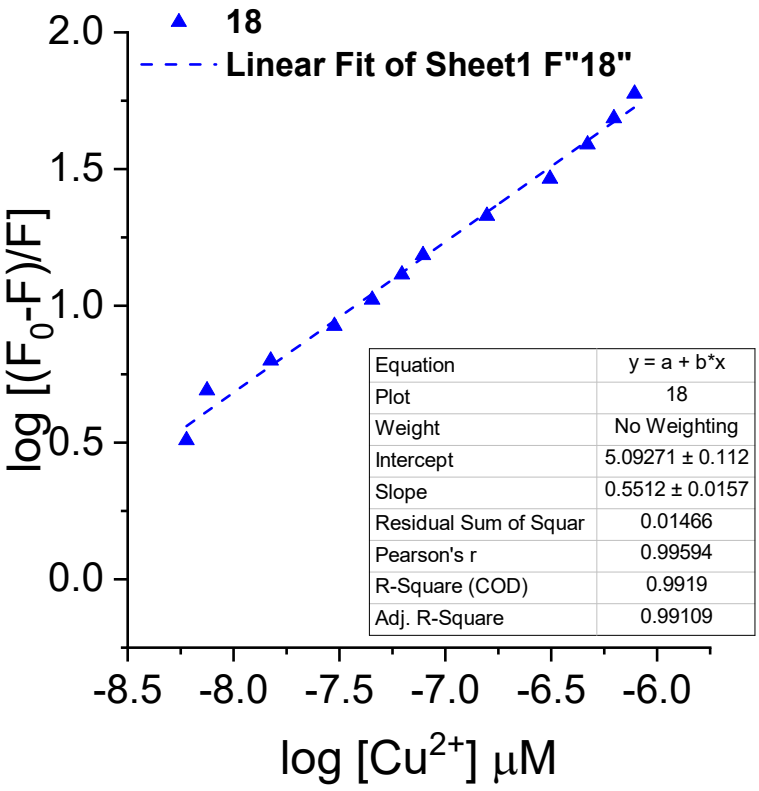

Fig. S28 Double logarithm plots for the K_a and *n* calculations of glycoconjugate **18**.

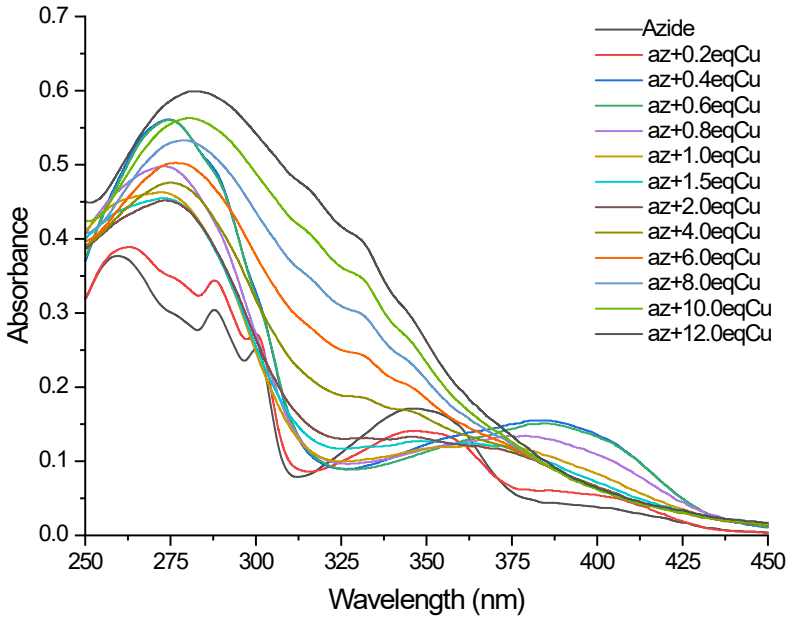

Fig. S29 UV-Vis absorption spectra of azide **3** (1.92×10^{-5} M) in the presence of different amounts of $Cu(NO_3)_2$.

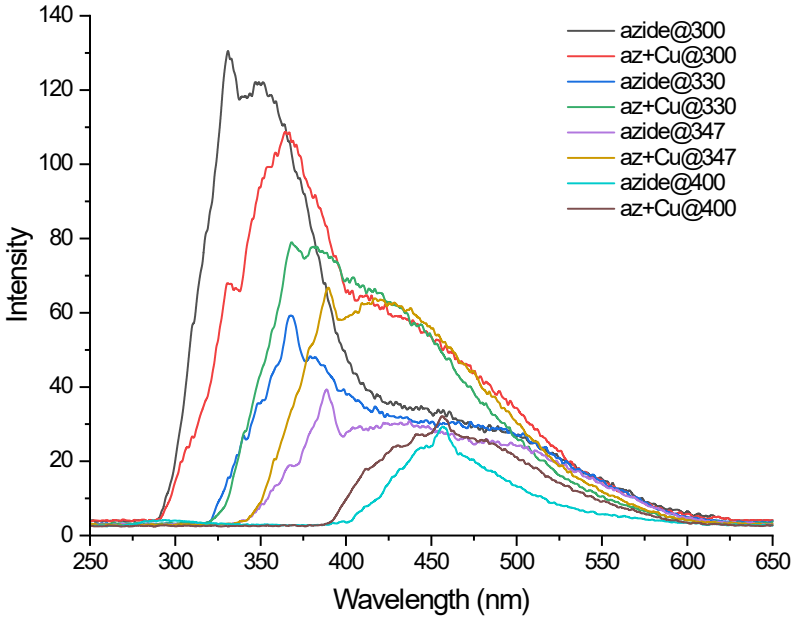

Fig. S30 Fluorescence emission spectra of azide **3** (1.92×10^{-5} M) at different excitation wavelengths in the presence of 12 equiv. of $Cu(NO_3)_2$.

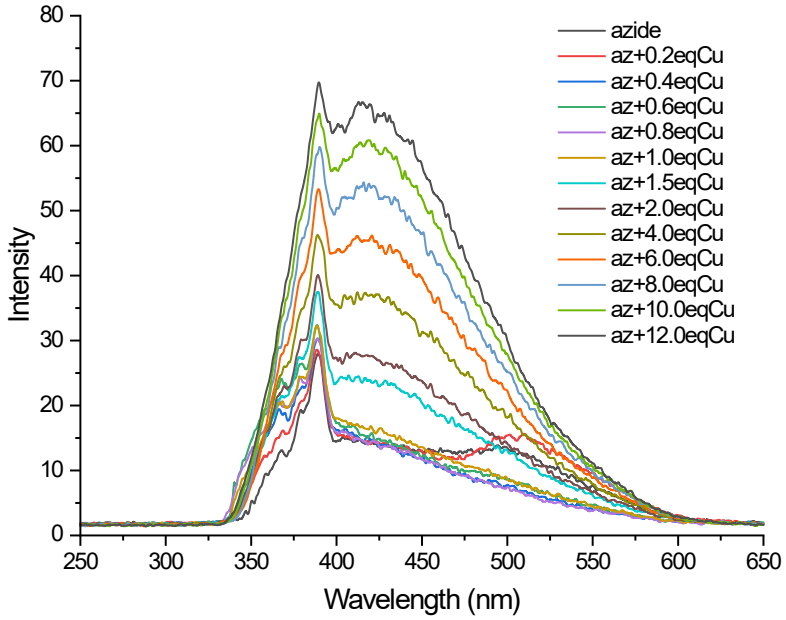

Fig. S31 UV-Vis absorption spectra of azide **3** ($1.92x10^{-5}$ M) in the presence of different amounts of $Cu(NO_3)_2$. (λ = 347 nm, Slit 5.0 nm/5.0 nm).

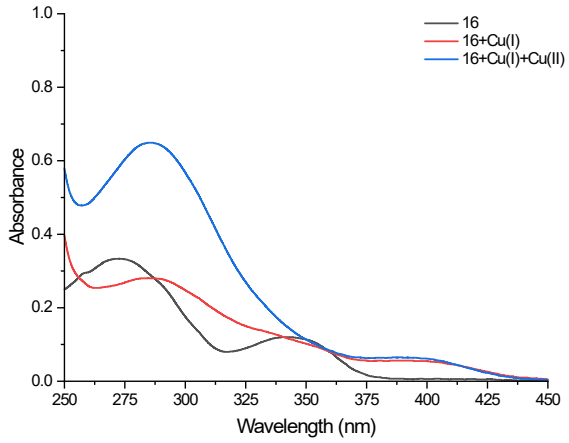

Fig. S31 UV-Vis spectra of glycoconjugate **16** ($1.92x10^{-5}$ M) after addition of Copper(I) and Copper(II). (Slit 5.0 nm/5.0 nm).

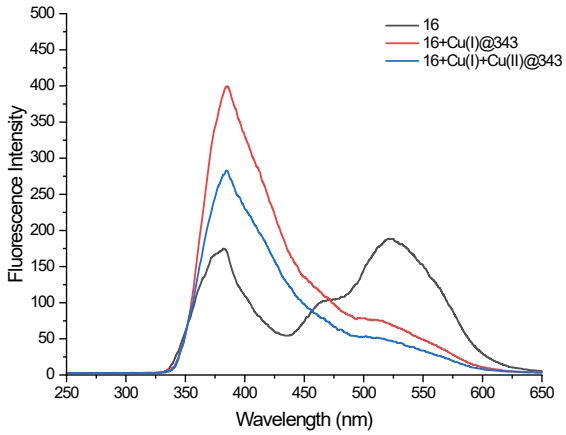

Fig. S32 Fluorescence emission spectra of glycoconjugate **16** (1.92×10^{-5} M) after addition of Copper(I) and Copper(II). (Slit 5.0 nm/5.0 nm).

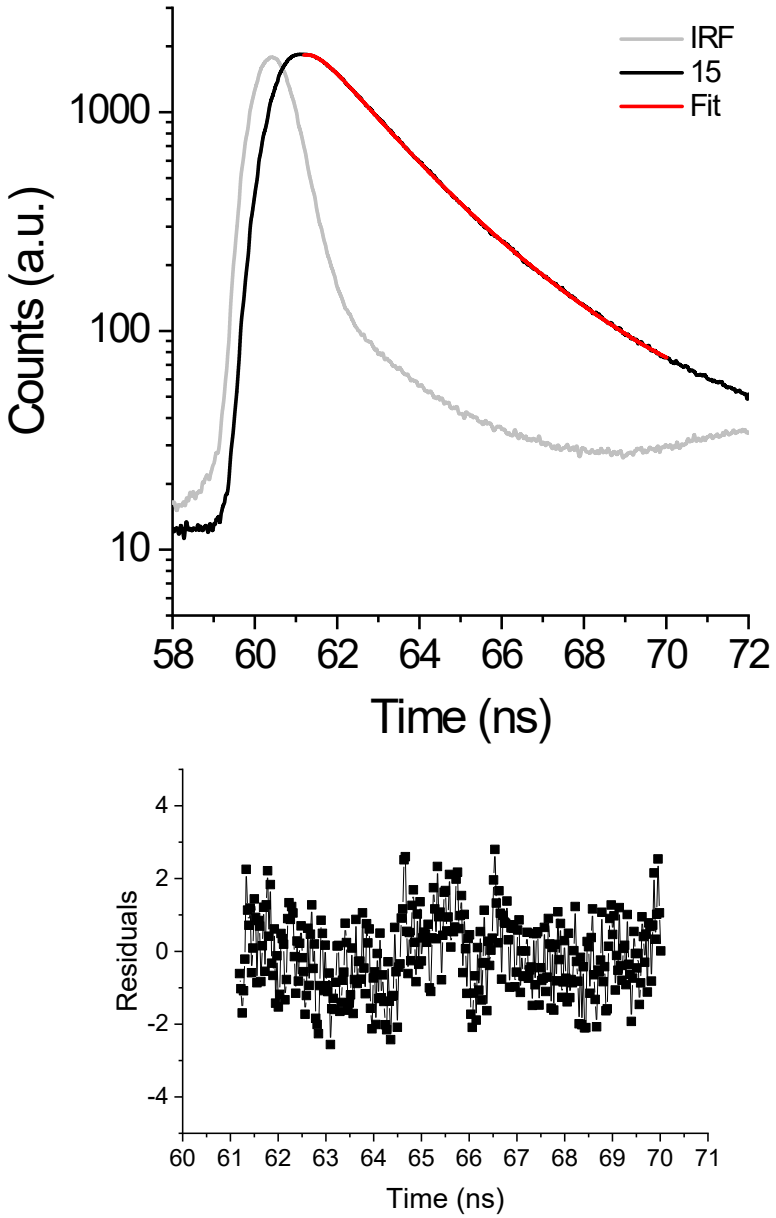

Fig. S33 Time-resolved fluorescence decay (λ_{exc}=330 nm) of the **15** in dichloromethane solution (~10^{-5} M), IRF (instrument response factor), and respective exponential fit. Below: Residuals from the exponential fit.

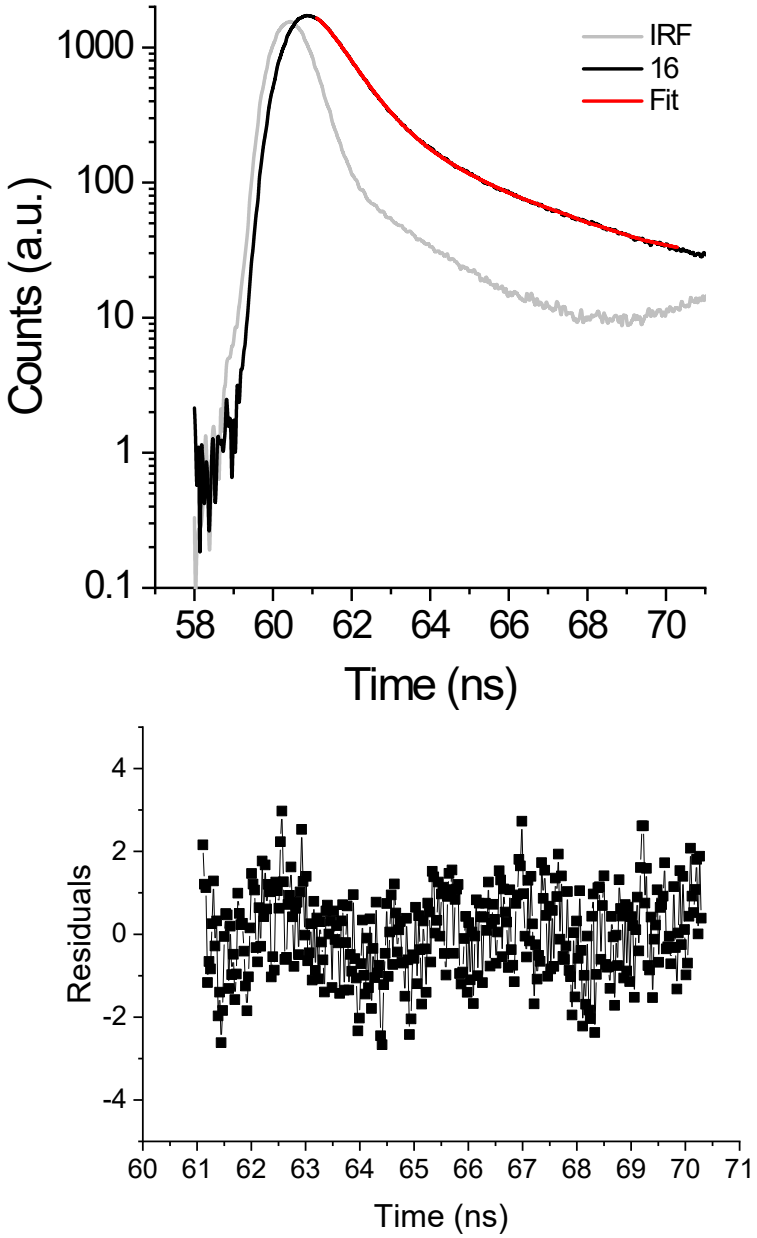

Fig. S34 Time-resolved fluorescence decay (λ_{exc}=330 nm) of the **16** in dichloromethane solution (~10^{-5} M), IRF (instrument response factor), and respective exponential fit. Below: Residuals from the exponential fit.

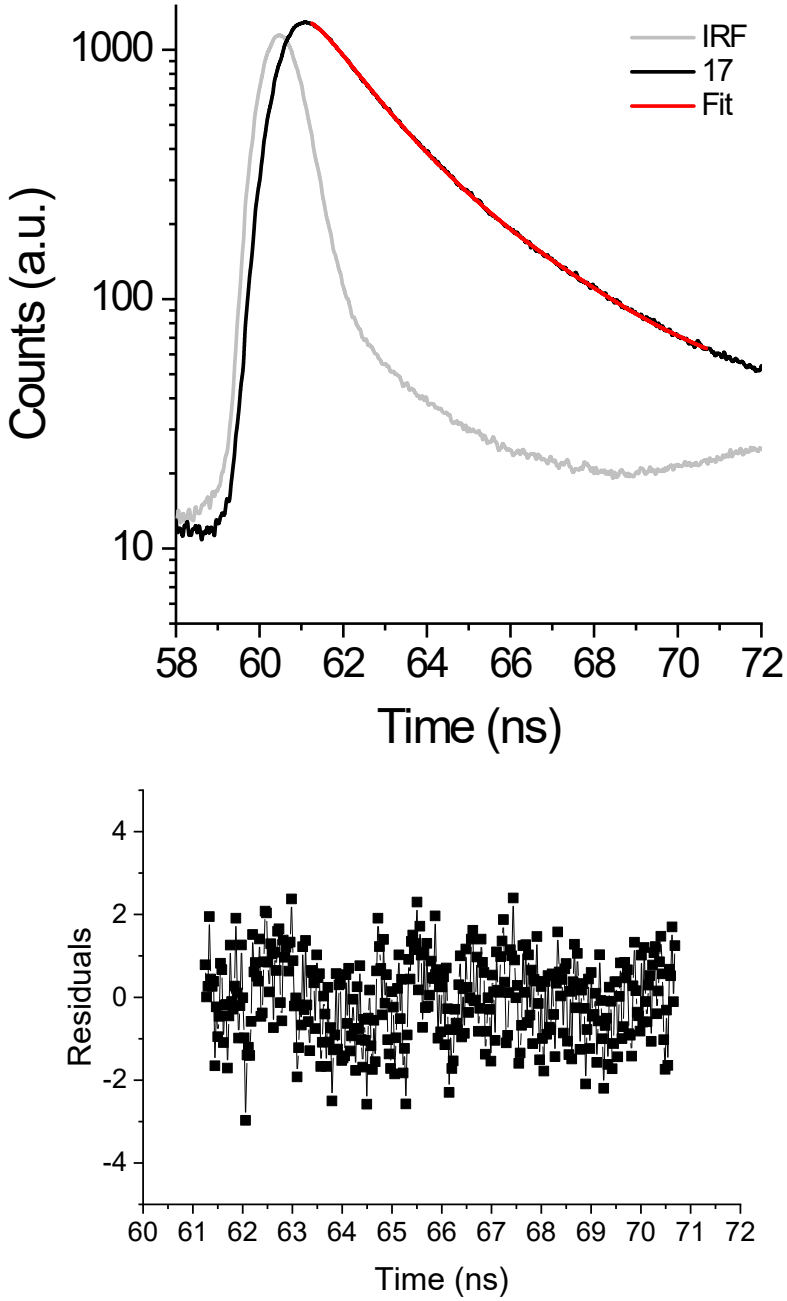

Fig. S35 Time-resolved fluorescence decay (λ_{exc}=330 nm) of the **17** in dichloromethane solution (~10^{-5} M), IRF (instrument response factor), and respective exponential fit. Below: Residuals from the exponential fit.

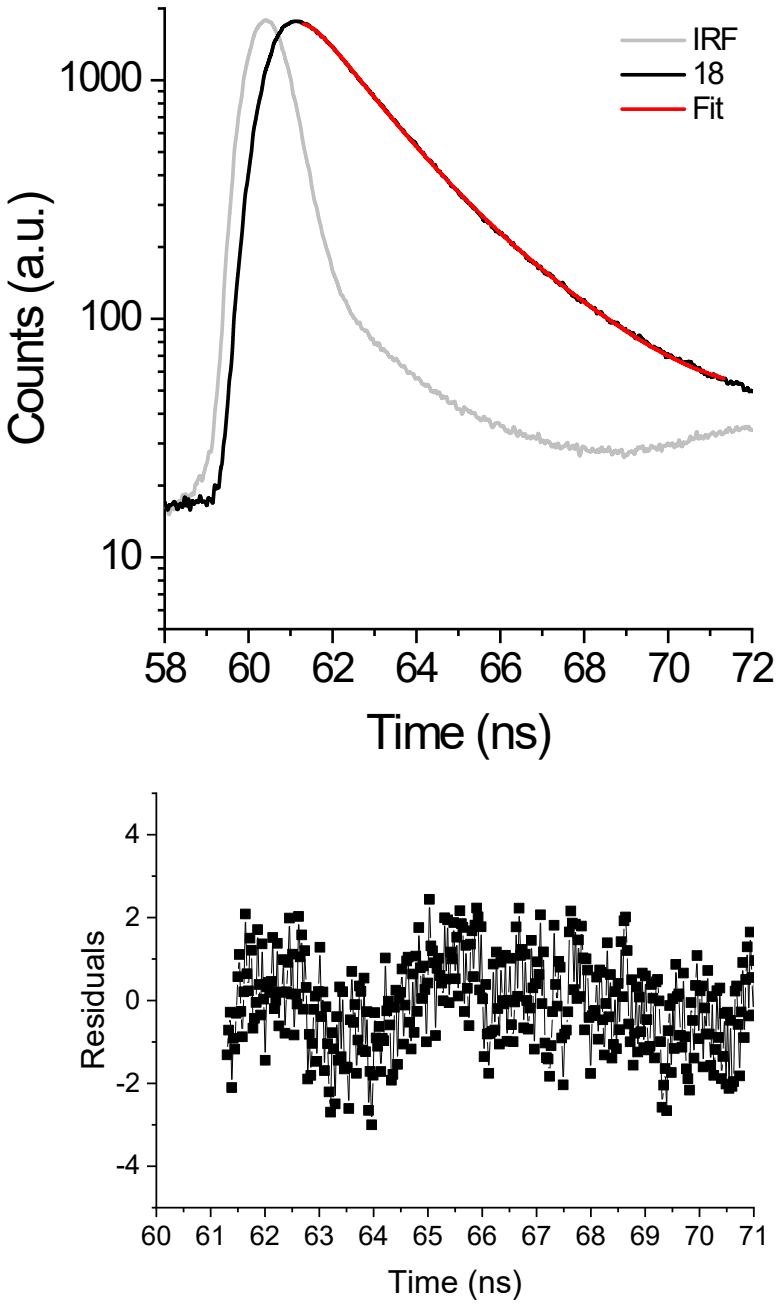

Fig. S36 Time-resolved fluorescence decay (λ_{exc}=330 nm) of the **18** in dichloromethane solution (~10^{-5} M), IRF (instrument response factor), and respective exponential fit. Below: Residuals from the exponential fit.

Time-resolved Spectroscopy data

****

Decay curve : Glycoconjugate 15
IRF curve : irf2

Start Time : 61.16
End Time : 70.04

Offset will be calculated
Shift will be calculated

Pre-exp. 1 : 1
Lifetime 1 : 1
Pre-exp. 2 : 1
Lifetime 2 : 1

***** Statistics *****

Job done after 181 iterations in 4.821 sec.

Fitted curve : FLD Fit (46)
Residuals : FLD Residuals (46)
Autocorrelation : FLD Autocorrelation (46)
Deconvolved Fit : FLD Deconvoluted (46)

Chi2 : 1.252
Durbin Watson : 1.359
Z : -0.07679

Pre-exp. 1 : 0.1464 ± 8.693e-003 (9.666± 0.5739%)
Lifetime 1 : 17.32 ± 1.523e+000
Pre-exp. 2 : 1.368 ± 4.825e-003 (90.33± 0.3185%)
Lifetime 2 : 1.554 ± 4.681e-003

F1 : 0.5438
F2 : 0.4562

Tau-av1 : 10.13
Tau-av2 : 3.078

Offset : -242.2
Shift : -0.1286

****

****
Decay curve : Glycoconjugate 16
IRF curve : irf

Start Time : 61.08
End Time : 70.32

Offset will be calculated
Shift will be calculated

Pre-exp. 1 : 1
Lifetime 1 : 1
Pre-exp. 2 : 1
Lifetime 2 : 1

***** Statistics *****

Job done after 90 iterations in 2.48 sec.

Fitted curve : FLD Fit (95)
Residuals : FLD Residuals (95)
Autocorrelation : FLD Autocorrelation (95)
Deconvolved Fit : FLD Deconvoluted (95)

Chi2 : 1.466
Durbin Watson : 1.421
Z : -0.01761

Pre-exp. 1 : 0.08194 ± 3.539e-003 (3.435 ± 0.1483%)
Lifetime 1 : 11.47 ± 1.365e+000
Pre-exp. 2 : 2.304 ± 9.299e-003 (96.57 ± 0.3898%)
Lifetime 2 : 0.7059 ± 3.590e-003

F1 : 0.3662
F2 : 0.6338

Tau-av1 : 4.646
Tau-av2 : 1.075

Offset : -59.87
Shift : 0.04997

****

****
Decay curve : Glycoconjugate 17
IRF curve : irf

Start Time : 61.22
End Time : 70.71

Offset will be calculated
Shift will be calculated

Pre-exp. 1 : 1
Lifetime 1 : 1
Pre-exp. 2 : 1
Lifetime 2 : 10

***** Statistics *****

Job done after 43 iterations in 1.295 sec.

Fitted curve : FLD Fit (25)
Residuals : FLD Residuals (25)
Autocorrelation : FLD Autocorrelation (25)
Deconvolved Fit : FLD Deconvoluted (25)

Chi2 : 1.085
Durbin Watson : 1.549
Z : -0.02834

Pre-exp. 1 : 1.51 ± 1.390e-002 (87.3 ± 0.8033%)
Lifetime 1 : 1.405 ± 1.059e-002
Pre-exp. 2 : 0.2198 ± 6.933e-003 (12.7 ± 0.4007%)
Lifetime 2 : 10.54 ± 1.202e+000

F1 : 0.4781
F2 : 0.5219

Tau-av1 : 6.174
Tau-av2 : 2.566

Offset : -148
Shift : 0.1835

****

****
Decay curve : Glycoconjugate 18
IRF curve : irf2

Start Time : 61.28
End Time : 71.36

Offset will be calculated
Shift will be calculated

Pre-exp. 1 : 1
Lifetime 1 : 1
Pre-exp. 2 : 1
Lifetime 2 : 1

***** Statistics *****

Job done after 100 iterations in 3.276 sec.

Fitted curve : FLD Fit (71)
Residuals : FLD Residuals (71)
Autocorrelation : FLD Autocorrelation (71)
Deconvolved Fit : FLD Deconvoluted (71)

Chi2 : 1.448
Durbin Watson : 1.437
Z : -0.04191

Pre-exp. 1 : 1.315 ± 5.797e-003 (89.71± 0.3953%)
Lifetime 1 : 1.487 ± 4.446e-003
Pre-exp. 2 : 0.1509 ± 7.659e-003 (10.29± 0.5223%)
Lifetime 2 : 18.82 ± 1.256e+000

F1 : 0.4079
F2 : 0.5921

Tau-av1 : 11.75
Tau-av2 : 3.271

Offset : -257.5
Shift : -0.1057

****

Additional Docking data

Table S1 The main amino acid residues and intermolecular forces for the interaction BSA-glycoconjugates **15-18** into site I of BSA.

Sample	Amino acid residues	Interaction	Distance (Å)
15	Trp-213	Hydrophobic	3.78
	Trp-213	Hydrogen bond	2.34
	Arg-217	Hydrogen bond	2.98
	Ser-342	Hydrophobic	3.51
	Ser-343	Hydrogen bond	2.10
	Leu-346	Hydrophobic	3.24
	Asp-450	Hydrogen bond	2.89
	Ser-453	Hydrogen bond	2.13
	Leu-480	Hydrophobic	3.26
16	Trp-213	Hydrogen bond	3.42
	Arg-217	Hydrogen bond	3.00
	Arg-217	π-cation	4.06
	Lys-294	Hydrogen bond	2.10
	Val-342 (peptidic bond)	Hydrogen bond	2.09
	Ser-343	Hydrogen bond	2.99
	Arg-483	Hydrophobic	3.62
17	Leu-197	Hydrophobic	3.34
	Ser-201	Hydrogen bond	2.10
	Trp-213	Hydrogen bond	2.50
	Arg-217	Hydrogen bond	2.86
	Arg-217	π-cation	4.15
	Glu-291	Hydrophobic	3.95
	Lys-294	Hydrogen bond	2.05
	Val-342 (peptidic bond)	Hydrogen bond	1.88
	Ser-343	Hydrogen bond	2.19
	Leu-346	Hydrophobic	3.38
	Leu-480	Hydrophobic	3.40
	Ser-453	Hydrogen bond	2.22
18	Trp-213	Hydrophobic	3.83
	Trp-213	Hydrogen bond	2.38
	Arg-217	Hydrogen bond	2.86
	Val-342	Hydrophobic	3.35
	Ser-343	Hydrogen bond	2.07
	Leu-346	Hydrophobic	2.95
	Arg-409	π-cation	4.72
	Lys-413	π-cation	3.40
	Asp-450	Hydrogen bond	3.30
	Ser-453	Hydrogen bond	2.09
	Leu-490	Hydrophobic	3.37